Article

Highly efficient dual-fibre optical trapping with 3D printed diffractive Fresnel lenses

Asa Asadollahbaik, Simon Thiele, Ksenia Weber, Aashutosh Kumar, Johannes Drozella, Florian Sterl, Alois Herkommer, Harald Giessen, and Jochen Fick

ACS Photonics, **Just Accepted Manuscript** • DOI: 10.1021/acsphotonics.9b01024 • Publication Date (Web): 17 Oct 2019

Highly efficient dual-fibre optical trapping with 3D printed diffractive Fresnel lenses

Asa Asadollahbaik,*,† Simon Thiele,‡ Ksenia Weber,† Aashutosh Kumar,¶ Johannes Drozella,‡ Florian Sterl,† Alois M. Herkommer,‡ Harald Giessen,† and Jochen Fick¶

†*4th Physics Institute and Research Center SCoPE, University of Stuttgart, Pfaffenwaldring 57, 70569, Stuttgart, Germany*

‡*Institute for Applied Optics and Research Center SCoPE, University of Stuttgart, Pfaffenwaldring 9, 70569 Stuttgart, Germany*

¶*Univ. Grenoble Alpes, CNRS, Grenoble INP, Institut Néel, 38000 Grenoble, France*

E-mail: a.asadollahbaik@pi4.uni-stuttgart.de

Abstract

Highly efficient counter-propagating fibre-based optical traps are presented which utilize converging beams from fibres with 3D printed diffractive Fresnel lenses on their facet. The use of converging beam instead of diverging beam in dual-fibre traps creates a strong trapping efficiency in both axial and transverse direction. Converging beams with a numerical aperture of up to 0.7 are produced by diffractive Fresnel lenses. These lenses also provide a large focal distance of up to 200μm in a moderately high refractive index medium. Fabrication of such diffractive lenses with micro-sized features at the tip of a fibre is possible by femtosecond two photon lithography. In comparison to chemically etched fibre tips, the normalized trap stiffness of dual-fibre tweezers is increased by a substantial factor of 35–50 when using converging beam produced by

diffractive Fresnel lenses. The large focal length provided by these diffractive structures allows to work at large fibre-to-fibre distance which leads to larger space and the freedom to combine other spectroscopy and analytical methods in combination with trapping.

Optical trapping was initially introduced by Ashkin[1] using two weakly diverging Gaussian laser beams with equal intensities in a counter-propagating arrangement. The optical trap is created on the beam axis and on a point of equal distance from the minimum waist of both beams where the radiation pressure is eliminated. Later, Ashkin succeeded in developing a single-beam optical trap in which scattering and gradient forces are balanced near the focus spot of a highly focused single-beam.[2] Through the years optical trapping found its way into a variety of applications such as microscopy,[3,4] biology,[5–10] nanotechnology,[11] etc. While single-beam optical traps are highly in demand due to their simplicity in using only one beam and consequently elimination of beam alignment, the bulky objectives necessary to provide the high numerical aperture (NA) are disadvantageous; their short working distance limits the free space around the trapped particle and makes it hard to integrate other manipulation and measurement processes to be performed simultaneously. These bulky optical components are also problematic with regard to flexibility of using optical traps for a variety of applications. In a dual-beam counter-propagating setup however, one can take advantage of the distance between the two beam sources and use a large working distance objective with a wide field of view for observation purposes or other spectroscopic measurements. Further advancements in this field also developed counter-propagating traps with more flexibility such as reconfigurable traps and mirror traps that can be used for the trapping of non-spherical nanoparticles or even high refractive index particles.[12–16] In order to miniaturize the trapping setup, laser beams and corresponding bulky optical components were replaced by the diverging beam of optical fibres and thus dual-fibre optical traps were developed.[17] In this arrangement, the particle is trapped in the middle of two equally powered optical fibres following the same principle as Ashkin's first counter-propagating trap.

In such dual-beam optical traps, whether using laser beams or fibres, different mechanisms lead to the trapping in transverse and axial direction. In transverse direction the gradient force has a more dominant role in comparison to the scattering force. The gradient forces of the two co-linear but counter-propagating beams work constructively and push the particle into the high intensity region, i.e. trapping spot. In axial direction, however, the low intensity diverging beam cannot create the gradient force required for trapping, and thus there is not much contribution from the gradient force. Stable trapping is formed between the two sources or fibre tips, where the two opposite scattering forces are cancelling each other. While such a setup is very sensitive to the alignment of fibres, a misalignment is not necessarily disadvantageous; controlled misalignment of fibres from the propagation axis can rotate the particle,[18,19] or changing the angle of the fibres with respect to each other can introduce off-axis trapping.[20,21]

One of the advantages of the use of weakly diverging beams is that it increases the trapping volume making it is easier for the particle to get trapped.[22] Such dual-fibre optical traps have proved to be suitable to trap micro-sized particles. This is based on the fundamental study that in counter-propagating arrangements the trap is stable only if the width of the beam at the trapping spot is larger than the diameter of the particle[23] which requires the beam to be divergent.[24] We have also previously used sharp tipped optical fibres in single and dual arrangements that can trap micro- and sub-micro sized particles.[25,26] However, since the trapping in the transverse direction is due to the gradient force, employing a more divergent beam to increase the trapping volume reduces the gradient force in the transverse direction and thus reduces the trapping stiffness.[27] As the trapping stiffness is reduced, the particle moves freely over a larger transverse distance and consequently over a larger volume.

In this work, we are using different beam intensity distributions for dual-fibre optical trapping: namely converging beams instead of diverging beams (Fig. 1a and 1b). Based on the fundamentals of conventional optical trapping, increasing the NA of a focused optical beam modifies the distribution of optical forces, especially in axial direction until an optical

trap is produced both in transverse and axial direction. If the NA is not large enough, the forces in axial direction are imbalanced and will push the particle away from the focal spot while in transverse direction a strong trapping effect could take effect due to gradient forces. This is known as 2D trapping, meaning that the particle is only trapped in transverse direction. Thus, an overlap of two identical 2D trapping spots can produce a focus region with additional trapping capabilities in the axial direction resulted by the equilibrium of forces of the two beams at their focal spot. In such an arrangement, since the focal length of the beam is known, the fibres should be kept at a distance equal to about twice the focal length of the focusing lens.

To create the focusing beam from the optical fibres the optical components have to be miniaturized to fit the dimensions of the fibre tip. However the performance of conventional spherical lenses deteriorates with increasing NA. Additionally, designing compact polymer optical components to achieve focusing with higher numerical apertures can be a challenging task if the devices are embedded into an immersion medium such as water. The low contrast in refractive index leads to lenses with extreme curvatures which are sensitive to fabrication tolerances. A viable alternative to purely refractive approaches are diffractive optical elements (DOEs) such as diffractive Fresnel lenses (also known as kinoform diffractive lenses[28] or échelette-type diffractive lenses[29]) which help to circumvent all the aforementioned drawbacks. Such structures also benefit from the flexibility of design in achieving a range of focal distance and numerical aperture which is beneficial to the field of optical trapping. Of such structures, surface plasmon lenses fabricated by metal deposition and subsequent electron beam nanostructuring as well as focused ion beam (FIB) milling,[30–32] Fresnel zone and phase plates by FIB milling,[33] and diffractive Fresnel lenses by nano-imprint lithography[34,35] are reported to add focusing capability to optical fibres. So far, Fresnel zone and phase plates and surface plasmon lenses have been used for 2D optical trapping in a single fibre arrangement.[32,33] However, diffractive Fresnel lenses on the tip of fibres have not been explored much and especially not for optical trapping.

Our diffractive Fresnel lenses are fabricated by femtosecond two photon lithography as a fast, reproducible, precise, and cost-efficient micro- and nano-scale fabrication technique.[34,36–44] This work evaluates the performance of 3D printed diffractive Fresnel lenses of three different NA, 0.3, 0.5, and 0.7 (with focal lengths of 200μm, 100μm and 50μm respectively) in dual-fibre setups for optical trapping (Fig. 1c). We demonstrate highly stable trapping at light powers as low as 220μW at the trapping spot for dielectric particles with diameters of 1μm and 500nm in water. Such setups with large fibre-to-fibre distances of 100–400μm are useful for single particle studies and single cell microscopy.

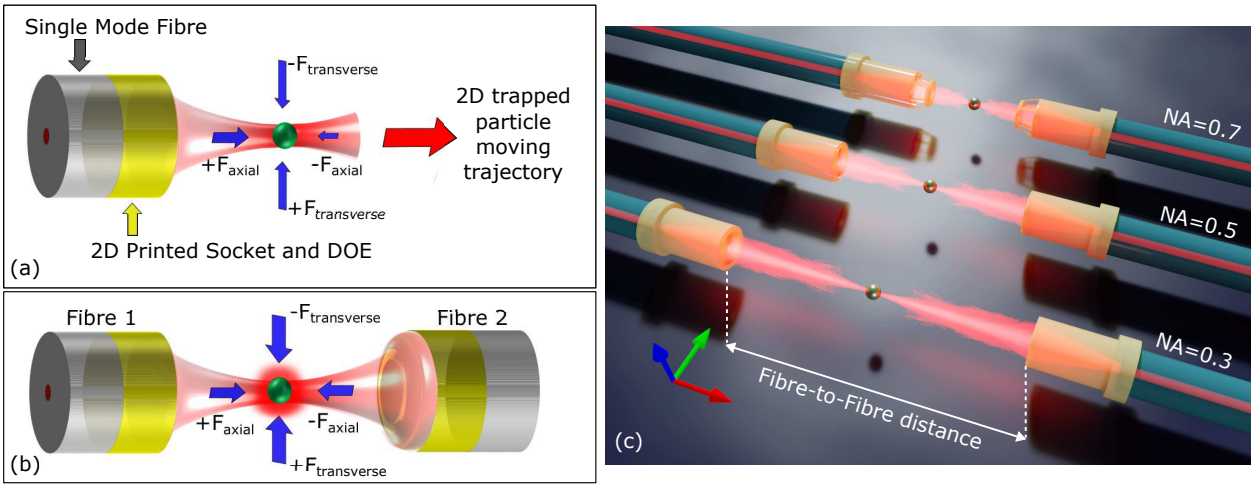

Figure 1: Force distribution and trapping condition by converging beams from 3D printed diffractive Fresnel lenses on fibres for (a) 2D trapping in a single fibre arrangement, and (b) 3D trapping in a dual-fibre arrangement. (c) Schematic of fibre-based counter-propagating optical tweezers, using single and doublet diffractive lenses at the tip of fibres with NA=0.3, 0.5 and 0.7 (focal length =200μm, 100μm and =50μm. Fibre-to-fibre distance is twice the focal length. The trapping wavelength is 808nm, and a range of optical powers from hundreds of μW up to 50mW are used (Dimensions are not up to scale).

Design and Fabrication

Diffractive lenses with three different numerical apertures of 0.3, 0.5, and 0.7 and respective focal lengths of 200μm, 100μm and 50μm in water were designed by the software ZEMAX (V.13, Zemax, LLC). The Gaussian beam exiting the fibre core with a wavelength of 808nm

is expanded by propagation through a solid cylinder with a length of 500μm called socket. An increased beam diameter is necessary to achieve reasonable working distances at high numerical apertures. The diffractive lenses are modelled via a phase function (in ZEMAX a so-called Binary 2 surface) and geometrical ray-tracing based on the local grating approximation. This surface type models the resulting phase shift $\phi(r)$ from the diffractive structure and defines it in terms of coefficients of a_i as $\phi(r) = \Sigma_{i=1}^{N} a_i.r^{2i}$. The optimized phase function $\phi(r)$ are then transferred into kinoform height profiles by the interference condition

$$z(r) = \frac{\lambda \cdot mod(\phi(r), 2\pi)}{2\pi(n_{resist} - n_{water})} \tag{1}$$

resulting in a profile height of 3.88μm. Even though the fabrication method allows for high aspect ratios of different segments, a lateral feature size of 1.67μm was selected as the minimum which is reached at the outer border of the design with a numerical aperture of 0.5. In order to realize an even higher numerical aperture of 0.7 the required diffractive power is distributed over two separated lenses with water in between. The second lens is held on top of the first lens by means of 6 pillars designed by mechanical design software (Fig. 2).

The polymer diffractive Fresnel lens structures are fabricated by femtosecond two photon lithography using a Photonic Professional GT (Nanoscribe GmbH) system. To accurately fabricate the high resolution features of the diffractive Fresnel lenses, the commercial IP-Dip resist[45] from Nanoscribe is chosen. The resist is applied directly to a 63× objective with high NA to produce the focused laser beam during the writing process. The fibre used in this work is a single mode fibre from Thorlabs (780HP) with cut-off wavelength at around 730nm that covers the wavelength of our laser source (808nm). The diameter of the cladding is 125μm and the mode field diameter is around 5 μm at $\lambda = 850$nm. The end of the fibre is stripped of its coating and a flat and clean facet is created by cleaving. The fibre is then inserted into the resist from the top, and aligned with the focal spot of the laser using the illuminated fibre core as a reference.[46] The beam expansion cylinder is fabricated with lower resolution

in slicing and hatching in comparison to the lens part to reduce writing time. Fast writing speeds of 50mm/s are possible with the use of the Galvo scanning system of the Nanoscribe machine. For the doublet lens, the pillars are written with the same parameters as the lenses. The total writing times are 50 minutes, 55 minutes, and 80 minutes for NA=0.3, and 0.5, and 0.7 respectively. Images of fabricated diffractive Fresnel lenses are provided in Fig. 2.

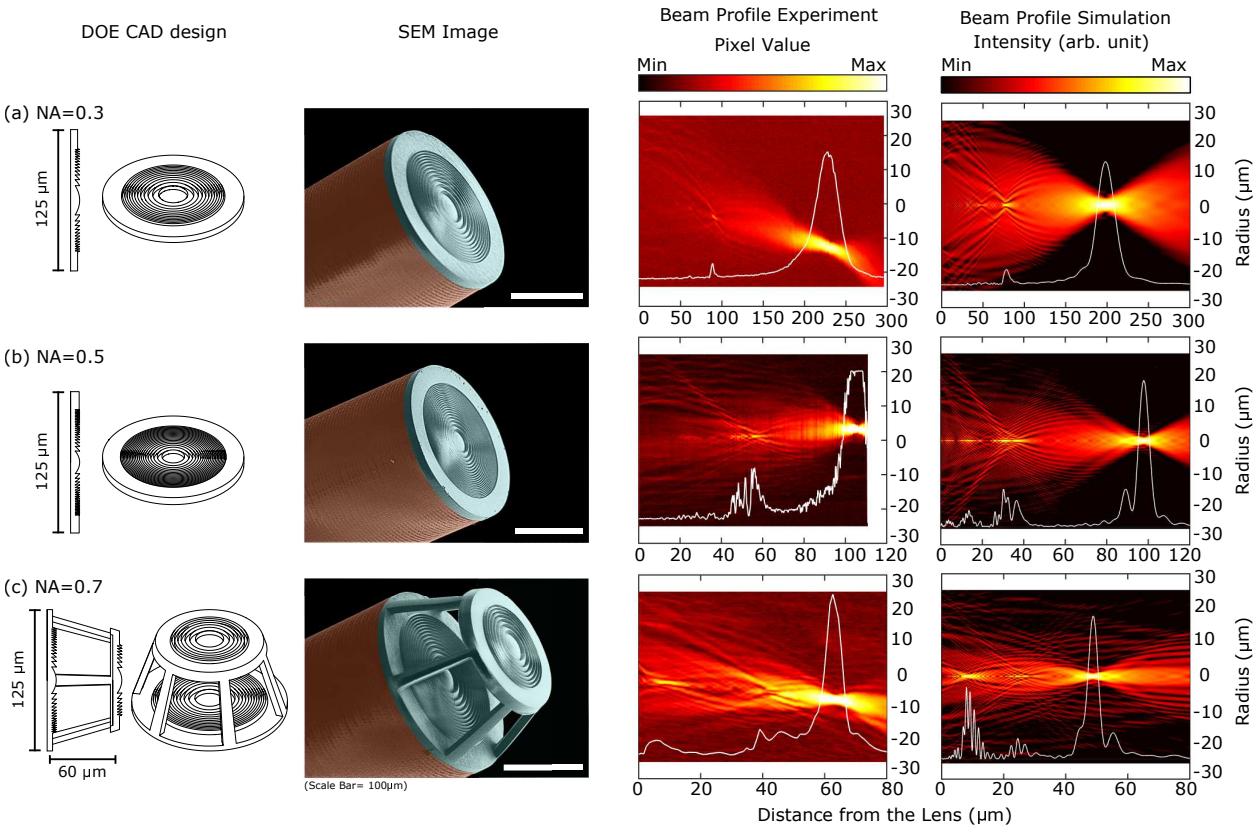

Figure 2: Computer aided design (CAD), false colour scanning electron microscope (SEM) image, and beam profile measurement (Experiment vs simulation) of fabricated diffractive Fresnel lenses on single mode fibres for (a) NA=0.3, (b) NA=0.5, and (c) NA=0.7, in water. The white line is an axial intensity cut at the centre of the beam with arbitrary units for both experimental and simulation diagram. (Surface plots are logarithmic values while the central intensity cuts (white lines) are from non-logarithmic data.)

In order to verify the performance of the fabricated lenses, we have performed a beam intensity profile imaging study in water, using an inverse microscope setup (Nikon Eclipse TE2000-U) and a water immersion objective (Nikon, APO LWD, 40x/1.15). In these measurements, the position of the microscope objective is moved along the optical axis from the

diffractive lens using a PIFOC piezo nanofocusing system from PI. A CCD imaging camera (Allied Vision GC2450c) is used to record an image for each position. From the resulting Z-stack, the beam intensity profile along the optical axis can be extracted. During the measurement, the creation of air bubbles on the surface of these lenses was observed, which could be a sign of hydrophobicity of the diffractive Fresnel lenses. These measurements are compared with an in-house wave optical simulation of the lenses using a volumetric Wave Propagation Method based on the Beam Propagation Method[47] (Fig. 2). Comparison of measured and simulated axial intensity distributions reveals good qualitative agreement with respect to the shape of the beam. There is a slight shift in the peak position which could be due to fabrication imperfections (curved diffractive features as opposed to sharp features),as well as a not perfectly matching refractive index. Additionally, the beam intensity measurement process could have potentially introduced some slight systematic length error. There is a slight tilt of the fibre during the measurement, however, the values of the horizontal axis are corrected while plotting the results.

Optical Trapping Setup

Details of the experimental setup are given in Ref. 25,48 . Briefly speaking, the dual-fibre optical trapping setup consists of two optical fibres with identical diffractive Fresnel lens facing each other. Each fibre is mounted on a set of xyz piezoelectric translation stages, allowing easy fibre alignment with sub-micrometer precision. The relative optical power of the 808nm trapping laser coupled into the two fibres is controlled by a half-wave plate and a polarizing beam splitter. Before and after trapping, the laser power is measured at each fibre tip in air. The values given in this paper correspond to the power emitted by each fibre with the corresponding diffractive lens.

Fibre-to-fibre optical transmission maps are recorded by scanning one of the two fibres in a plane normal to the fibre axis. These maps are used to optimize the fibre alignment and

to determine the optimum fibre-to-fibre distance. Details of this process are provided in the supplementary section.

Particle trapping is visualized by a custom made microscope using a 50× large working distance objective together with a CMOS camera. Trapping videos containing typically 5000 frames have been recorded at $\sim$ 300fps. Particle position tracking is realized using an in-house algorithm in the free Scilab environment.[49] In this algorithm the particle position is determined by fitting a two-dimensional Gaussian function, resulting in an improved spatial resolution with respect to the camera resolution of 96 nm/pixel. The particle positions in axial and transverse directions with respect to the fibre axis are recorded separately.

The trap stiffness κ is subsequently determined applying Boltzmann statistics (BS) in the framework of the equipartition theorem and power spectra analysis (PSA) as described in detail in Ref. 48. In this context, κ corresponds to the spring constant of the harmonic oscillator model applied to describe the trapping potential. In the case of BS, κ is obtained by fitting the particle position probability to the Gaussian function $P(r) = \exp(-\kappa r^2/2k_BT)$, with k_B as Boltzmann constant and T the temperature. In the case of PSA, κ is obtained by fitting the particle position power spectra to the Lorentz function:

$$P_k = \frac{2k_BT}{\gamma_0(f_c^2 + f_k^2)} \tag{2}$$

with $f_c = \kappa/2\pi\gamma_0$ the corner frequency, $\gamma_0 = 6\pi\eta a$ and f_k the oscillation frequency from the Fourier transform.[50] The Lorentz fit of the power spectra (Eq. 2) has three distinct features (in the log–log presentation): (i) a constant low frequency region ($P_k^{low} = 8\pi^2 k_BT\gamma_0/\kappa^2$), (ii) a high frequency linear negative slope ($P_k^{high} = 2k_BT/\gamma_0 f_k^2$), and (iii) the characteristic or corner frequency ($f_c = \kappa/2\pi\gamma_0$) separating (i) and (ii). Only the first and third feature depend on the trap stiffness. The negative slope can, however, be useful in order to verify the validity of the model.

Results

Optical Trapping of 1μm Particle in Water

Optical trapping of 1μm polystyrene particles has been successfully performed for all three available fibre lens types. The applied fibre-to-fibre distances for the NA=0.3, 0.5, and 0.7 fibres are d=385, 195, and 125μm respectively which is close to twice the nominal focal lengths. A series of successive trapping experiments at different light powers is performed for each lens type. Stable trapping was observed at very low power; for the singlet diffractive lens with NA = 0.5 the lowest power was 220μW. An example of a trapping video with NA = 0.5 is attached in the supplementary material.

The position tracking results of three representative trapping experiments are displayed in Fig. 3. The trapping efficiency is significantly different for the three diffractive Fresnel lenses. Most efficient trapping is observed for the lens with an NA of 0.5. In this case, the particle is confined in a volume of approximately 150×1300nm^2. For the lens with NA of 0.3 the particle is trapped in a much larger, but still highly anisotropic volume. Finally the trapping volume becomes nearly spherical for the doublet lens with NA 0.7. The time dependent position records (Fig. 3 (d-f)) show that the oscillation in axial direction is not homogeneous, but that the particle trajectory is composed of relatively slow drift and higher frequency oscillations.

As explained before, the strong trapping observed here is explained by the optical forces of different nature in axial and transverse directions resulted by overlapping the two focal spots of the same diffractive lens that can only provide a 2D optical trap if used in a single fibre arrangement. In the axial direction, the opposing forces of the two laser beams are pushing the particle into the trap center. Small perturbations of this equilibrium result in relatively large particle displacements. In the transverse direction the gradient force attracts the particle into the beam axis. For the two beams these forces are acting in the same direction, resulting in a very efficient particle trapping.

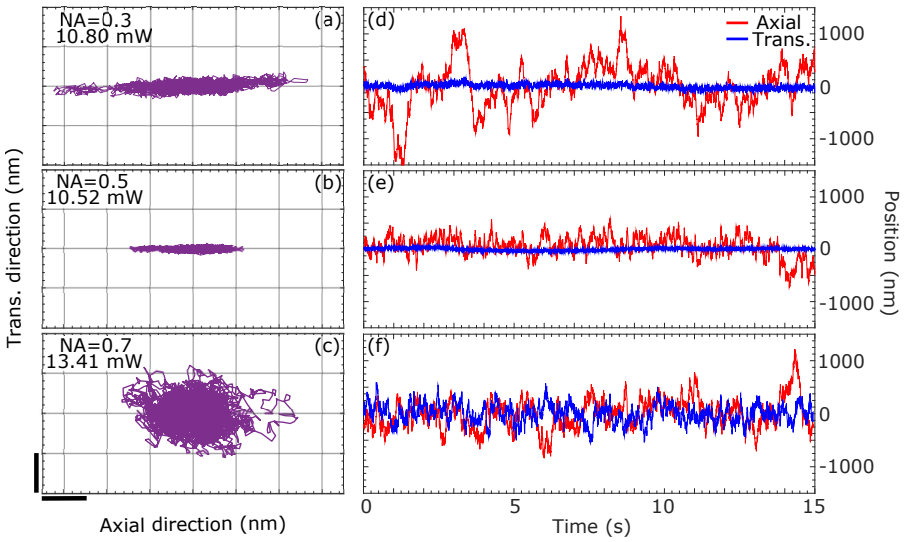

Figure 3: Position tracking for three representative trapping experiments, for diffractive Fresnel lenses with NA=0.3, 0.5 and 0.7. (a-c) represents the position tracking in space (scale bar is 500nm), (d-f) represents the time dependent position tracking in axial and transverse direction.

The trapping efficiency of the optical tweezers is determined by calculating the trapping stiffness κ using BS (Fig. 4) as well as PSA (Fig. 5).

In the case of the BS method, the anisotropic trapping potential results in a larger position distribution in the axial direction. Considering a harmonic trapping potential, the position distribution is described by a Gaussian function. This condition is verified for most of the transverse curves of the experimental results with one exception at the highest power for the lens with NA=0.5 in which a two peak distribution is observed (Fig. 4c, pink line). In the axial direction, experimental results do not fit very well to a Gaussian function. In this case, two distinct situations are observed: one with two meta-stable trapping positions (e.g. NA 0.5 @ 6.35mW) and another with an arbitrary distribution with a large width (e.g. NA 0.3 @ 24.2mW).

Considering the data for the PSA model, there exists an acceptable fit between the data and the Lorenz function in the transverse direction for all three lens types at low laser powers. For higher powers, the power spectra fitted values at low frequencies are not coherent with the corner frequency. In such cases, for each measurement only the frequency

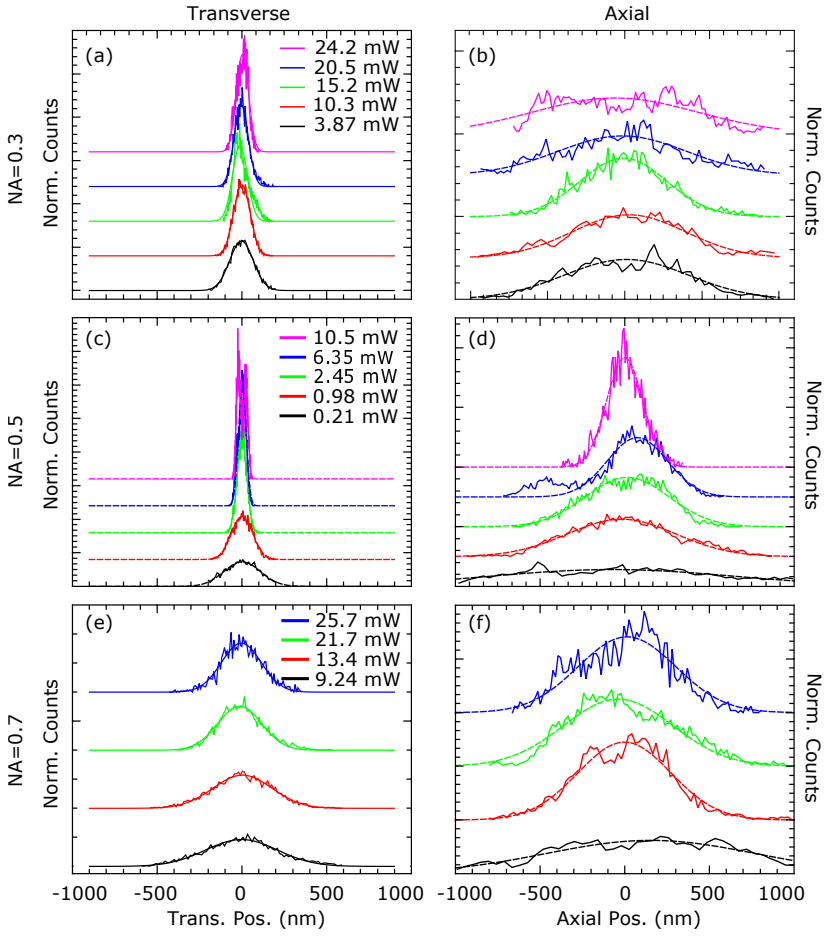

Figure 4: Position Distribution vs Laser Power for the calculation of trapping efficiency using BS method. Results are presented in the order of transverse (left) and axial (right) direction and for diffractive lenses with (a and b) NA=0.3, (c and d) NA=0.5, and (e and f) NA=0.7. Dashed lines present the best Gaussian function fit.

region that is fitting the data is considered. Moreover, for frequencies below approximately 7 – 10 Hz the power spectra is increasing with decreasing frequencies. In axial direction, there is a good degree of fitting between experimental results and the model. The relatively low trapping efficiencies result in low corner frequencies close to the lower frequency limits of the measurements. The trapping efficiency values obtained by numerical fitting to the experimental results show some uncertainty. The very good fitting to the high frequency slope underlines the quality of the experimental results, however does not contribute to deduce the trapping efficiency values.

During measurements, a high peak at ≈ 68.5 Hz is observed for all cases. For the most efficient trap configuration (NA=0.5 @ 10.5 mW, in transverse direction) this peak represents the maximum particle displacement. Its low amplitude of about 50nm (for 1μm particles) and the consistency of its value for several experiments with different fibres and optical powers, suggests that this feature is due to the vibration of the optical setup and irrelevant to the optical trapping measurement.

Analysis of Trapping Experiments

All experimental trap stiffness values (κ) are summarized in Fig. 6. In this figure, filled-in symbols represent measurements with a good fit to the model, whereas the hollow symbols are only partially fitting as described above. The lines are obtained by linear fitting to the confident points. Their slope corresponds to the normalized trap stiffness $\tilde{\kappa}$ in terms of power as summarized in Tab. 1. It is an important point to mention that the light power values in this paper correspond to the total emitted power from each fibre type in air. Relating these values to the power in the trapping spot is not straightforward. First, a significant fraction of the power is scattered by the diffractive lenses and second, trapping is done in water. Transmission measurements in air and water of two identical fibres (NA=0.5) indicate that the effective emission in water is about 1.4 times smaller than in air. As a result the actual light power at the trapping position is at least 1.4 times lower than

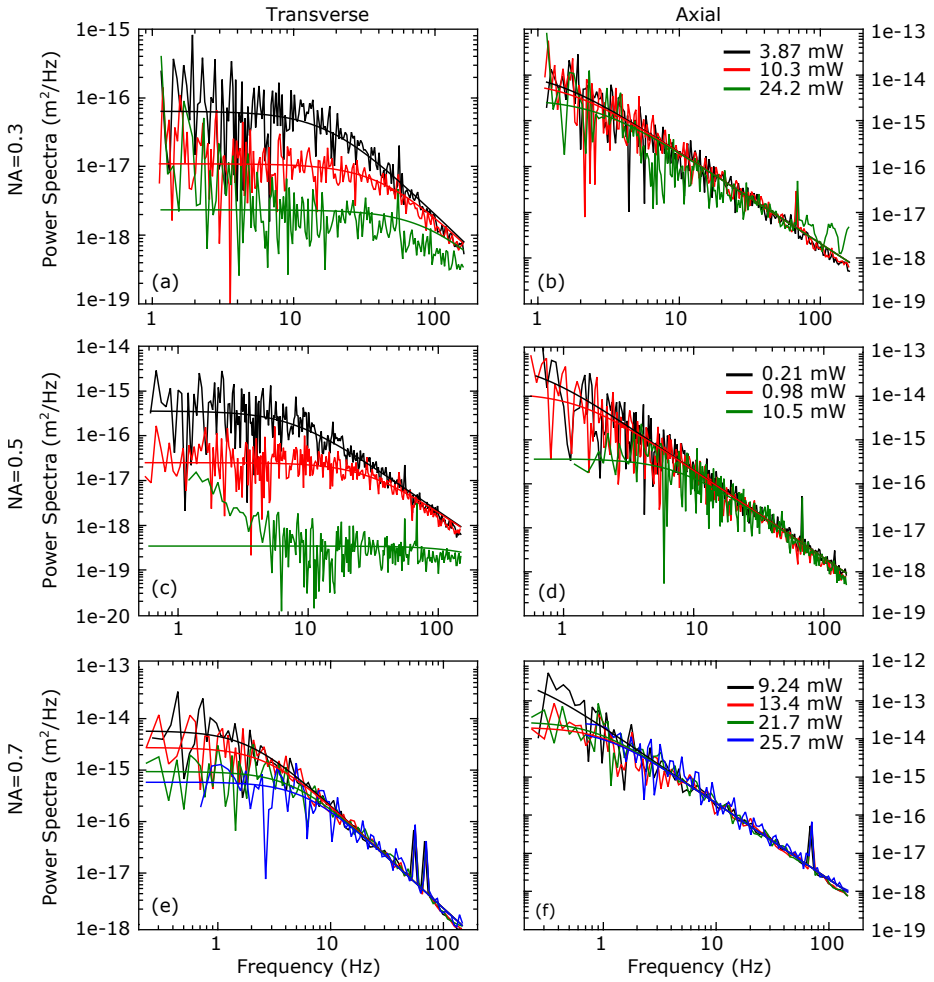

Figure 5: Power Spectra vs Frequency for the calculation of trapping efficiency using PSA method. Results are presented in the order of transverse (left) and axial (right) direction and for lenses with (a and b) NA=0.3, (c and d) NA=0.5, and (e and f) NA=0.7. Bold lines are best numerical fits to the Lorentz function of Eq. 2.

presented here. Consequently, the normalised trapping efficiency ($\tilde{\kappa}$) is also higher than the values presented here. However, as the exact correction is difficult to obtain, we prefer to present the uncorrected values.

In general the stiffness values obtained by Boltzmann statistics are lower than the values obtained by power spectra analysis with very significant differences. This discrepancy is due to the fact that BS integrates the particle motion over the entire video duration. A slow particle drift (can be observed in Fig. 3) enlarges the position distribution. For random movements the Gaussian fitting is still possible, but underestimates the actual κ value. For experiments in which the particle is moving between two meta-stable positions (e.g. NA=0.5 @ 10.5mW, in transverse direction in Fig. (4)), a Gaussian fit with multiple peaks is resulted. Thus a meaningful definition of κ is not anymore possible and in Fig. 6 the corresponding values are marked as non-confident (hollow symbols) or even omitted. It is believed that these two meta-stable trapping positions are due to pseudo focal spots created by diffractive beams from lenses at higher power.

In the case of PSA, the slow particle drift (Fig. 3) affects only the low frequency region and explains the power spectra increase for frequencies below 10 Hz. Neglecting these frequencies during fitting results in higher κ values in comparison to the BS method. The normalized trapping efficiency ($\tilde{\kappa}$) values obtained by taking the slope of the linear fit to κ values from PSA (Tab. 1), are in very good agreement with the values calculated from the low-power measurements with a good fit to the Lorentzian model.

The highest trapping efficiency is observed for the diffractive Fresnel lens with NA=0.5 in axial direction with $\tilde{\kappa} = 1762.87$ pN.μm^{-1}·W^{-1}. This value is about 35 to 50 times higher than similar measurements using chemical wet-etched fibre tips with quasi-Bessel[51] or Gaussian[48] beam emission respectively. Moreover, trapping at light powers as low as 220μW is possible for a fibre-to-fibre distance of 195μm , which can be beneficial for adding other functions to optical trapping.

Trapping with diffractive lens with NA = 0.3 is less efficient, but still has higher stiffness

values in comparison to previous results with etched optical fibre tips. In this case the very large fibre-to-fibre distance of nearly 400μm can be of great interest for trapping experiments in complex environments.

Finally trapping with doublet diffractive lenses with NA=0.7 is significantly less efficient than the two other lens types. This result can be explained by the more complex structure of these doublet lenses in terms of fabrication and the creation of bubbles between the doublet lenses and consequent problems found for perfectly wetting the inner space between the two lenses.

Table 1: Normalized trap stiffness $\tilde{\kappa}$ in (pN$\cdot\mu m^{-1}\cdot$W^{-1}) using three diffractive Fresnel lens types and obtained by power spectra analysis (PSA) and Boltzmann statistics (BS) (NA: numerical aperture of the diffractive lens, d_{f-f}: fibre-to-fibre distance, $d_{particle}$: trapped particle diameter).

NA	d_{f-f} (μm)	$d_{particle}$ (μm)	$\tilde{\kappa}_{transverse}$		$\tilde{\kappa}_{axial}$	
			PSA	BS	PSA	BS
0.3	385	1.0	268.15	127.67	13.52	3.11
0.5	195	1.0	1762.87	1217.57	50.51	31.31
0.7	125	1.0	13.32	10.55	2.6	1.9
0.5	195	0.5	28.20	34.95	3.28	2.07

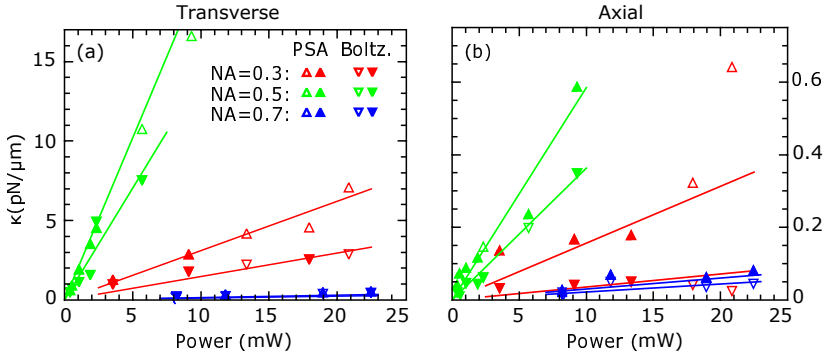

Figure 6: Trap stiffness in (a) transverse and (b) axial directions, calculated by PSA (upward triangles) and BS (downward triangles) for diffractive lenses with NA=0.3, 0.5 and 0.7 at different laser powers. The filled-in symbols represent values with an acceptable fit, and hollow symbols represent values with less acceptable fits.

Optical Trapping of 500 nm Particles

In a further series, polystyrene particles with 500nm diameter are trapped with the diffractive lenses with NA=0.5 to highlight their outstanding performance. The experimental values are $\tilde{\kappa}^{PSA} = 28.2$ and 3.28 pN$\cdot\mu m^{-1}\cdot$W^{-1} in transverse and axial directions respectively (Tab. 1).

By slight misalignment of the two fibres, the trapped particle starts oscillating at about 10Hz on a slightly tilted elliptical orbit with axial and transverse amplitudes of respectively 3.5 and 0.3μm (Fig. 7). In the present configuration, the proportionality of particle speed (v) and optical force allows to calculate the optical force by $F_{opt} = \gamma_0 v$.[52] The maximum obtained force is about 1.9 pN for a light power of 27.75mW.

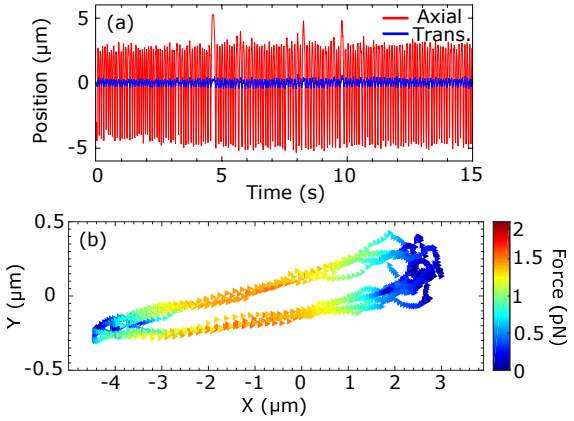

Figure 7: Oscillating movement of 500nm diameter particle in the dual-fibre trap with DOE lenses of NA=0.5 lens with slightly misaligned fibres. The trapped particle oscillates at about 10 Hz on a slightly tilted elliptical orbit with axial and transverse amplitudes of respectively 3.5 and 0.3μm.

Discussion

Based on the above results, one can see that these traps are highly stable with large fibre-to-fibre distance and low laser power as their highlighting properties. By using converging beams for dual propagating optical trapping instead of diverging beams, strong trapping in both transverse direction (due to gradient forces) and axial direction (due to strong axial

forces) are created. This is the first time such optical traps with converging beams for micro-sized objects are created and used.

The first point to mention is that designing optical components to provide such a wide variation of numerical aperture from 0.3 to 0.7 is made possible by using DOEs and in particular diffractive Fresnel lenses. Design investigations of an aspherical lens with NA=0.48 showed that, due to the extension of the structure in axial direction, the free working distance had to be reduced from 100μm to 40μm compared to the DOE version with the same diameter. Additionally, in contrast to binary diffractive lenses, our diffractive Fresnel lenses suppress light in unwanted diffraction orders through their continuous design of the zone profiles. Thus, diffraction efficiencies (proportion of light at the focal position) approaching 100% can be achieved at low NA and well above 50% at higher NA.

Based on conventional optical trapping, one might expect that the trapping stiffness increases with increasing the designed NA. However, it has to be considered that in DOEs a part of the light is diffracted into unwanted diffraction orders leading to extra peaks even in case of a perfect diffractive Fresnel profile. In all cases the focus of the first diffraction order contains most of the energy and is located very close to the z-position of the geometric design. As expected, the design with NA=0.7 leads to the smallest full-width at half-maximum (FWHM). This smaller focus spot provides a less stable trapping spot for the particle with the diameter of 1μm. Consequently, the trap stiffness does not show a linear behaviour with respect to increasing NA.

The key feature of the high trapping efficiency of the diffractive lens with NA equal to 0.5 is due to its ability to produce a more concentrated laser focus in axial direction. The authors had previously designed and fabricated an aspherical lens on fibres with NA of 0.3. Using such fibres in similar trapping experiments, only resulted transient particle trapping of one or (up to) ten axially aligned particles. Transmission measurements between the two aspherical lensed fibres show a minimum spot waist of 3.3μm for a fibre-to-fibre distance of 380μm. Comparing these values to a waist of 1μm for a fibre-to-fibre distance of

200μm for the lens with NA=0.5, the stronger focusing leads to higher light intensities and a smaller trapping region (especially in axial direction), explaining the outstanding trapping efficiencies of our diffractive Fresnel lenses. This feature was, in principle, confirmed by straightforward theoretical considerations based on the dipolar approximation. Comparing the two lens types, the maximum optical force was found to be ∼14 times higher and the trapping region about ∼15 times narrower for our diffractive Fresnel lenses.

Conclusion

We have demonstrated highly efficient three dimensional optical trapping in counter-propagating fibre arrangement by using converging beams instead of diverging beams. Highly efficient trapping with stiffnesses of up to 1762 pN.μm^{-1}.W^{-1} at low laser power of 220μW are achieved at a large fibre-to-fibre distance equal to twice the focal length of the diffractive lenses. Converging beams with low to moderate NA of 0.3 to 0.7 are produced by 3D printed diffractive Fresnel lenses at the tip of fibres. The advantage of using such diffractive elements in comparison to aspherical lenses is their capability of producing a variety of NAs with higher working distances, as well as ease of fabrication. The highly accurate trapping spot with high stiffness can be beneficial for single cell and single particle microscopy as well as particle manipulation. This successful demonstration of optical trapping by diffractive Fresnel lenses on fibres shows the great potential of microstructured optical fibres that can be used for optical trapping and micro-manipulation.

Acknowledgement

We gratefully acknowledge financial support by the BMBF (Printoptics, Q.Link.X), BW Stifung (Opterial), DFG(SPP1839 and 1929), ERC(Complexplus), ERCPoC (3D Printedoptics), National Science Foundation (NSF) (1253236, 0868895, 1222301), Program 973 (2014AA014402), French National Research Agency (ANR-16-CE24-00-01). We would like

to furthermore thank Mr Tobias Pohl for his valuable help with graphics, and Ms Kim-Miriam Baar from Nikon for lending us the water immersion objective to perform our beam profile intensity measurements in water.

Supporting Information Available

The following supplementary are available:

- Trapping video file with diffractive Fresnel lens with NA=0.5, particle diameter=1μm,
- Dual-fibre alignment process,
- Numerical simulations of optical trapping forces.

References

(1) Ashkin, A. Acceleration and Trapping of Particles by Radiation Pressure. *Phys. Rev. Lett.* **1970**, *24*, 156–159.

(2) Ashkin, A.; Dziedzic, J. M.; Bjorkholm, J. E.; Chu, S. Observation of a single-beam gradient force optical trap for dielectric particles. *Opt. Lett.* **1986**, *11*, 288–290.

(3) Ghislain, L. P.; Webb, W. W. Scanning-force microscope based on an optical trap. *Optics Letters* **1993**, *18*, 1678–1680.

(4) Lee, W. M.; Reece, P. J.; Marchington, R. F.; Metzger, N. K.; Dholakia, K. Construction and calibration of an optical trap on a fluorescence optical microscope. *Nature protocols* **2007**, *2*, 3226.

(5) Ashkin, A.; Schütze, K.; Dziedzic, J.; Euteneuer, U.; Schliwa, M. Force generation of organelle transport measured in vivo by an infrared laser trap. *Nature* **1990**, *348*, 346.

(6) Block, S. M.; Goldstein, L. S.; Schnapp, B. J. Bead movement by single kinesin molecules studied with optical tweezers. *Nature* **1990**, *348*, 348.

(7) Molloy, J. E.; Padgett, M. J. Lights, action: optical tweezers. *Contemporary physics* **2002**, *43*, 241–258.

(8) Bustamante, C.; Bryant, Z.; Smith, S. B. Ten years of tension: single-molecule DNA mechanics. *Nature* **2003**, *421*, 423.

(9) Zhang, H.; Liu, K.-K. Optical tweezers for single cells. *Journal of The Royal Society Interface* **2008**, *5*, 671–690.

(10) Dholakia, K.; Reece, P.; Gu, M. Optical micromanipulation. *Chemical Society Reviews* **2008**, *37*, 42–55.

(11) Maragò, O. M.; Jones, P. H.; Gucciardi, P. G.; Volpe, G.; Ferrari, A. C. Optical trapping and manipulation of nanostructures. *Nature nanotechnology* **2013**, *8*, 807.

(12) van der Horst, A.; van Oostrum, P. D.; Moroz, A.; van Blaaderen, A.; Dogterom, M. High trapping forces for high-refractive index particles trapped in dynamic arrays of counterpropagating optical tweezers. *Applied optics* **2008**, *47*, 3196–3202.

(13) Pitzek, M.; Steiger, R.; Thalhammer, G.; Bernet, S.; Ritsch-Marte, M. Optical mirror trap with a large field of view. *Optics express* **2009**, *17*, 19414–19423.

(14) Zwick, S.; Haist, T.; Miyamoto, Y.; He, L.; Warber, M.; Hermerschmidt, A.; Osten, W. Holographic twin traps. *Journal of Optics A: Pure and Applied Optics* **2009**, *11*, 034011.

(15) Čižmár, T.; Brzobohatỳ, O.; Dholakia, K.; Zemánek, P. The holographic optical micromanipulation system based on counter-propagating beams. *Laser Physics Letters* **2010**, *8*, 50.

(16) Donato, M. G.; Brzobohaty, O.; Simpson, S. H.; Irrera, A.; Leonardi, A. A.; Lo Faro, M. J.; Svak, V.; Marago, O. M.; Zemánek, P. Optical trapping, optical binding, and rotational dynamics of silicon nanowires in counter-propagating beams. *Nano letters* **2018**, *19*, 342–352.

(17) Constable, A.; Kim, J.; Mervis, J.; Zarinetchi, F.; Prentiss, M. Demonstration of a fiber-optical light-force trap. *Opt. Lett.* **1993**, *18*, 1867–1869.

(18) Black, B. J.; Luo, D.; Mohanty, S. K. Fiber-optic rotation of micro-scale structures enabled microfluidic actuation and self-scanning two-photon excitation. *Applied Physics Letters* **2012**, *101*, 221105.

(19) Xu, X.; Cheng, C.; Xin, H.; Lei, H.; Li, B. Controllable orientation of single silver nanowire using two fiber probes. *Scientific reports* **2014**, *4*, 3989.

(20) Liberale, C.; Cojoc, G.; Bragheri, F.; Minzioni, P.; Perozziello, G.; La Rocca, R.; Ferrara, L.; Rajamanickam, V.; Di Fabrizio, E.; Cristiani, I. Integrated microfluidic device for single-cell trapping and spectroscopy. *Scientific reports* **2013**, *3*, 1258.

(21) Ti, C.; Thomas, G. M.; Ren, Y.; Zhang, R.; Wen, Q.; Liu, Y. Fiber based optical tweezers for simultaneous in situ force exertion and measurements in a 3D polyacrylamide gel compartment. *Biomedical optics express* **2015**, *6*, 2325–2336.

(22) Lyons, E. R.; Sonek, G. J. Confinement and bistability in a tapered hemispherically lensed optical fiber trap. *Applied Physics Letters* **1995**, *66*, 1584–1586.

(23) Roosen, G. A theoretical and experimental study of the stable equilibrium positions of spheres levitated by two horizontal laser beams. *Optics Communications* **1977**, *21*, 189–194.

(24) Guck, J.; Ananthakrishnan, R.; Moon, T.; Cunningham, C.; Käs, J. Optical deformability of soft biological dielectrics. *Physical review letters* **2000**, *84*, 5451.

(25) Decombe, J.-B.; Valdivia-Valero, F. J.; Dantelle, G.; Leménager, G.; Gacoin, T.; Des Francs, G. C.; Huant, S.; Fick, J. Luminescent nanoparticle trapping with far-field optical fiber-tip tweezers. *Nanoscale* **2016**, *8*, 5334–5342.

(26) Leménager, G.; Lahlil, K.; Gacoin, T.; Des Francs, G. C.; Fick, J. Optical fiber tip tweezers, a complementary approach for nanoparticle trapping. *Journal of Nanophotonics* **2018**, *13*, 012505.

(27) Sidick, E.; Collins, S. D.; Knoesen, A. Trapping forces in a multiple-beam fiber-optic trap. *Applied optics* **1997**, *36*, 6423–6433.

(28) Moreno, V.; Román, J. F.; Salgueiro, J. R. High efficiency diffractive lenses: Deduction of kinoform profile. *American Journal of Physics* **1997**, *65*, 556–562.

(29) Lalanne, P.; Chavel, P. Metalenses at visible wavelengths: past, present, perspectives. *Laser & Photonics Reviews* **2017**, *11*, 1600295.

(30) Taguchi, K.; Ueno, H.; Ikeda, M. Rotational manipulation of a yeast cell using optical fibres. *Electronics Letters* **1997**, *33*, 1249–1250.

(31) Liu, Y.; Xu, H.; Stief, F.; Zhitenev, N.; Yu, M. Far-field superfocusing with an optical fiber based surface plasmonic lens made of nanoscale concentric annular slits. *Optics express* **2011**, *19*, 20233–20243.

(32) Liu, Y.; Stief, F.; Yu, M. Subwavelength optical trapping with a fiber-based surface plasmonic lens. *Opt. Lett.* **2013**, *38*, 721–723.

(33) Ribeiro, R. S. R.; Dahal, P.; Guerreiro, A.; Jorge, P. A.; Viegas, J. Fabrication of Fresnel plates on optical fibres by FIB milling for optical trapping, manipulation and detection of single cells. *Scientific reports* **2017**, *7*, 4485.

(34) Koshelev, A.; Calafiore, G.; Piña-Hernandez, C.; Allen, F. I.; Dhuey, S.; Sassolini, S.; Wong, E.; Lum, P.; Munechika, K.; Cabrini, S. High refractive index Fresnel lens on a

fiber fabricated by nanoimprint lithography for immersion applications. *Optics letters* **2016**, *41*, 3423–3426.

(35) Koshelev, A.; Calafiore, G.; Pina-Hernandez, C.; Allen, F. I.; Dhuey, S.; Sassolini, S.; Wong, E.; Lum, P.; Cabrini, S.; Munechika, K. *Advanced Fabrication Technologies for Micro/Nano Optics and Photonics XI*; 2018; Vol. 10544; p 105440A.

(36) LaFratta, C. N.; Fourkas, J. T.; Baldacchini, T.; Farrer, R. A. Multiphoton fabrication. *Angewandte Chemie International Edition* **2007**, *46*, 6238–6258.

(37) Gan, Z.; Cao, Y.; Evans, R. A.; Gu, M. Three-dimensional deep sub-diffraction optical beam lithography with 9 nm feature size. *Nature communications* **2013**, *4*, 2061.

(38) Gissibl, T.; Thiele, S.; Herkommer, A.; Giessen, H. Two-photon direct laser writing of ultracompact multi-lens objectives. *Nature Photonics* **2016**, *10*, 554.

(39) Gissibl, T.; Schmid, M.; Giessen, H. Spatial beam intensity shaping using phase masks on single-mode optical fibers fabricated by femtosecond direct laser writing. *Optica* **2016**, *3*, 448–451.

(40) Thiele, S.; Gissibl, T.; Giessen, H.; Herkommer, A. M. Ultra-compact on-chip LED collimation optics by 3D femtosecond direct laser writing. *Optics letters* **2016**, *41*, 3029–3032.

(41) Thiele, S.; Arzenbacher, K.; Gissibl, T.; Giessen, H.; Herkommer, A. M. 3D-printed eagle eye: Compound microlens system for foveated imaging. *Science advances* **2017**, *3*, e1602655.

(42) Gissibl, T.; Thiele, S.; Herkommer, A.; Giessen, H. Sub-micrometre accurate free-form optics by three-dimensional printing on single-mode fibres. *Nature communications* **2016**, *7*, 11763.

(43) Schmid, M.; Thiele, S.; Herkommer, A.; Giessen, H. Three-dimensional direct laser written achromatic axicons and multi-component microlenses. *Optics letters* **2018**, *43*, 5837–5840.

(44) Weber, K.; Hütt, F.; Thiele, S.; Gissibl, T.; Herkommer, A.; Giessen, H. Single mode fiber based delivery of OAM light by 3D direct laser writing. *Optics express* **2017**, *25*, 19672–19679.

(45) Gissibl, T.; Wagner, S.; Sykora, J.; Schmid, M.; Giessen, H. Refractive index measurements of photo-resists for three-dimensional direct laser writing. *Opt. Mater. Express* **2017**, *7*, 2293–2298.

(46) Giessen, H.; Thiel, M.; Gissibl, T. Method and device for producing microstructures on optical fibers. 2018; US Patent App. 15/765,914.

(47) Schmidt, S.; Tiess, T.; Schröter, S.; Hambach, R.; Jäger, M.; Bartelt, H.; Tünnermann, A.; Gross, H. Wave-optical modeling beyond the thin-element-approximation. *Optics Express* **2016**, *24*, 30188–30200.

(48) Decombe, J.-B.; Huant, S.; Fick, J. Single and dual fiber nano-tip optical tweezers: trapping and analysis. *Opt. Express* **2013**, *21*, 30521–30531.

(49) Scilab Enterprises, Scilab: Free and Open Source software for numerical computation. Scilab Enterprises: Orsay, France, 2012.

(50) Berg-Sørensen, K.; Flyvberg, H. Power spectrum analysis for optical tweezers. *Rev. Sci. Instrum.* **2004**, *75*, 594–612.

(51) Decombe, J.-B.; Mondal, S.; Kumbhakar, D.; Sarkar Pal, S.; Fick, J. Single and multiple micro-particle trapping using non-Gaussian beams from optical fiber nano-antennas. *Selected Topics in Quantum Electronics, IEEE Journal of* **2015**, *21*, 1–6.

(52) Fick, J. Out-of-equilibrium force measurements of dual-fiber optical tweezers. *Opt. Lett.* **2016**, *41*, 5716–5719.

Graphical TOC Entry

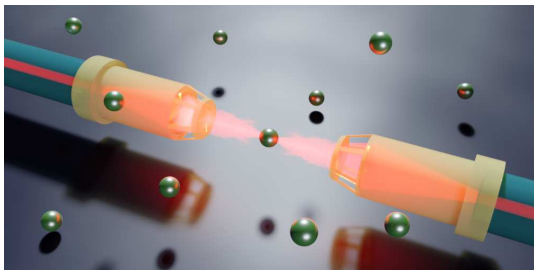

For the Table of Contents use only.